Process-fidelity estimation of a linear optical quantum-controlled-*Z* gate: A comparative study

M. Mičuda, M. Sedlák, I. Straka, M. Miková, M. Dušek, M. Ježek, and J. Fiurášek

Department of Optics, Palacký University, 17. listopadu 1192/12, CZ-771 46 Olomouc, Czech Republic

(Received 30 January 2014; published 7 April 2014)

We present a systematic comparison of different methods of fidelity estimation of a linear optical quantum-controlled-*Z* gate implemented by two-photon interference on a partially polarizing beam splitter. We utilize a linear fidelity estimator based on the Monte Carlo sampling technique as well as a nonlinear estimator based on maximum likelihood reconstruction of a full quantum-process matrix. In addition, we evaluate the lower bound on quantum-gate fidelity determined by average quantum-state fidelities for two mutually unbiased bases. In order to probe various regimes of operation of the gate we introduce a tunable time delay between the two photons. This allows us to move from high-fidelity operation to a regime where the photons become distinguishable and the success probability of the scheme significantly depends on the input state. We discuss in detail possible systematic effects that could influence the gate-fidelity estimation.

I. INTRODUCTION

Most quantum-computation and quantum-information processing schemes rely on devices that transform quantum states while preserving their purity and quantum coherence. For example, in the quantum-circuit model of computation the elementary steps of the computation, quantum gates, are intended to be unitary transformations. Ideally, the gates should operate deterministically according to a given prescription and the goal of the experimentalist is to approach this regime as closely as possible. However, the experimentally implemented gates always deviate somewhat from the ideal ones due to various practical imperfections, thus creating some general transformation, a quantum channel. In some types of experiments, e.g., in quantum optics, the implementation of the gate may even be probabilistic and as a consequence the actually implemented transformation is a general probabilistic quantum operation.

Motivated by the need to benchmark the experimentally implemented quantum gates and to identify their errors and imperfections, the development of tools for experimental characterization of quantum operations has attracted considerable attention in recent years. Several approaches have been proposed that differ in terms of the required resources as well as in the amount of information they provide. Often we want to understand precisely how the gate operates and we want to know exactly all of its imperfections. Quantum-process tomography [1–4] serves exactly this purpose and provides us with the full description of the gate, for example, in terms of its Choi operator χ [5–7]. However, a complete quantum tomography requires resources that grow exponentially with the number of qubits unless one can assume that the Choi matrix χ has a small rank r, in which case one can apply compressed sensing [8,9]. This motivated the search for other efficient methods of quantum-gate characterization, whose goal is to determine only some specific features of the gate. Typically, we wonder how close the actual gate is to the ideal one and as a measure we use quantum-process fidelity.

It was shown by Hofmann that the quantum-process fidelity can be efficiently bounded by measuring the average quantum-state fidelities for two mutually unbiased bases [10,11]. This procedure has received considerable attention and has been

utilized in several experiments to estimate the fidelity of a quantum-CNOT gate [12–17], Toffoli gate [18], and multiqubit unitary operations on qubits carried by trapped ions [19]. If one wants to determine the exact value of the gate fidelity without performing full quantum-state tomography, one can resort to the Monte Carlo sampling techniques [20–24]. The main advantage of Monte Carlo sampling is that the fidelity estimation error depends on the number of measurements and not on the size of the system, which makes this approach particularly suitable for characterization of operations on large numbers of qubits. However, even for small-scale systems the Monte Carlo sampling may reduce the number of measurements below that required for full quantum-process tomography.

In this paper we present a systematic comparison of different methods of fidelity estimation of a linear optical quantum-controlled-*Z* (CZ) gate. In the computational basis, this two-qubit gate introduces π phase shift if and only if both qubits are in state $|1\rangle$,

$$U_{\mathrm{CZ}} = |00\rangle\langle00| + |01\rangle\langle01| + |10\rangle\langle10| - |11\rangle\langle11|. \quad (1)$$

Recall that the CZ gate is equivalent to the CNOT gate up to a single-qubit Hadamard transform on the target qubit. We have performed full quantum-process tomography of the gate and we have also estimated the quantum-process fidelity by Monte Carlo sampling and determined the Hofmann lower bound on the process fidelity. A peculiar feature of the linear optical quantum gates is that they are probabilistic [25], hence they generally need to be described by trace-decreasing quantum maps and the success probability of such a gate may depend on the input state. Recently, we showed that the Hofmann bound is applicable to such probabilistic operations, but the average state fidelities have to be calculated as weighted means with weights equal to the relative success probabilities for each input probe state [18]. Here we explicitly demonstrate that by using the ordinary state averages instead of the weighted ones one could actually overestimate the gate fidelity. Since the Hofmann bound has been applied in the past to characterize probabilistic linear optical CNOT gates in several experiments, we investigate in depth the influence of unequal success probabilities on the fidelity bounds.
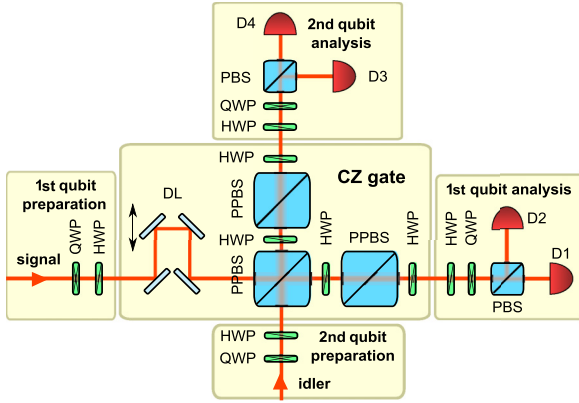
FIG. 1. (Color online) Experimental setup: PPBS denotes partially polarizing beam splitter; PBS, polarizing beam splitter; HWP, half-wave plate; QWP, quarter-wave pate; D, single-photon detector; and DL, tunable temporal delay line.

For this purpose we deliberately introduce a tunable temporal delay between two photons whose polarization states represent the qubits on which the gate acts. By changing this delay we can move from high-fidelity operation, where success probabilities for all input states are almost equal, to a regime where the photons become distinguishable and the success probabilities exhibit significant variations. We find that our experimental results are generally in agreement with theoretical expectations. Nevertheless, we observe certain minor differences between the fidelity estimates determined by full process tomography and by Monte Carlo sampling that are larger than statistical uncertainty. Also, in the high-visibility regime we find that the Hofmann lower bound apparently slightly exceeds the estimated gate fidelity. We discuss possible systematic effects that could influence the performance of the gate and explain these discrepancies.

The rest of the paper is organized as follows. The experimental setup is described in Sec. II. The quantum-process-fidelity estimation methods are reviewed in Sec. III. In Sec. IV we describe a simple theoretical model that shows how the fidelity of a linear optical CZ gate depends on the visibility of two-photon interference. Experimental results are presented and discussed in Sec. V. Finally, Sec. VI contains a brief summary and conclusions.

II. EXPERIMENTAL SETUP

We employ time-correlated photon pairs generated in the process of frequency-degenerate spontaneous parametric down-conversion in a 2-mm-long β barium borate crystal cut for type-II phase matching and pumped with a continuous-wave laser diode with a central wavelength of 405 nm and 110 mW of power [26]. The orthogonally polarized signal and idler photons are spatially separated at a polarizing beam splitter, coupled into single-mode fibers, and released back into free space at the input of the experimental setup shown in Fig. 1. Qubits are encoded into polarization states of the photons and an arbitrary state of each qubit can be prepared using a sequence of quarter-wave plates and half-wave plates. Computational basis states are associated with horizontal and vertical polarizations as $|0\rangle \equiv |H\rangle$ and $|1\rangle \equiv |V\rangle$, respectively. Besides the computational basis states we also use diagonally and antidiagonally linearly polarized states

$$|D\rangle = \frac{1}{\sqrt{2}}(|H\rangle + |V\rangle), \quad |A\rangle = \frac{1}{\sqrt{2}}(|H\rangle - |V\rangle), \quad (2)$$

as well as the left- and right-hand circularly polarized states

$$|R\rangle = \frac{1}{\sqrt{2}}(|H\rangle + i|V\rangle), \quad |L\rangle = \frac{1}{\sqrt{2}}(|H\rangle - i|V\rangle). \quad (3)$$

The quantum CZ gate is implemented by two-photon interference on a partially polarizing beam splitter (PPBS) that fully transmits horizontally polarized photons ($T_H = 1$) while it partially reflects vertically polarized photons ($T_V = 1/3$) [12,27–31]. The two-photon interference on the PPBS results in a π phase shift if and only if both photons are vertically polarized, i.e., in logical state $|1\rangle$. The scheme also requires two additional PPBSs for balancing the amplitudes. Since all three partially polarizing beam splitters in our setup have the same splitting ratios, we use additional half-wave plates rotated at 45° to flip the horizontal and vertical polarizations. This ensures that the sequence of the central PPBS and the auxiliary PPBS acts as a polarization-insensitive filter with effective transmittance 1/3 for all polarizations. This linear optical gate operates in the coincidence basis [30] and its success is indicated by simultaneous detection of a single photon at each output port. The gate is thus inherently conditional and its theoretical success probability reads 1/9.

Polarization states of both output photons were analyzed by standard polarization measurement blocks consisting of a half-wave plate, a quarter-wave plate, a polarizing beam splitter, and single-photon detectors. In order to avoid the need to precisely calibrate relative detection efficiencies of the single-photon detectors, we have used only two-photon coincidences between a single pair of detectors D2 and D3 for further data processing. Two-photon coincidences corresponding to measurement in any chosen product two-qubit basis were thus recorded sequentially and the measurement time of each number of coincidences was set to 30 s.

III. FIDELITY ESTIMATION METHODS

For our purposes, a quantum operation $\mathcal{E}$ is most conveniently described using the Choi-Jamiolkowski isomorphism [5,6], which attributes to each completely positive map $\mathcal{E}$ a positive semidefinite operator χ on a tensor product of input and output Hilbert space. This operator can be intuitively defined as a density matrix of a quantum state obtained by applying the operation $\mathcal{E}$ to one part of a pure maximally entangled state $|\Phi^+\rangle$ on two copies of an input Hilbert space

$$\chi = \mathcal{I} \otimes \mathcal{E}(\Phi^+), \quad (4)$$

where $\mathcal{I}$ denotes the identity operation and $\Phi^+ = |\Phi^+\rangle\langle\Phi^+|$ denotes a density matrix of the pure state $|\Phi^+\rangle$. For two-qubit operations we explicitly have

$$|\Phi^+\rangle = \sum_{j,k=0}^{1} |jk\rangle|jk\rangle. \quad (5)$$

An input density matrix ρ_{in} is transformed by $\mathcal{E}$ into $\rho_{\text{out}} = \mathcal{E}(\rho_{\text{in}})$, which can be expressed as

$$\rho_{\text{out}} = \text{Tr}_{\text{in}}\big[\rho_{\text{in}}^T \otimes \mathbb{I}_{\text{out}} \chi\big], \qquad (6)$$

where T stands for the transposition in the computational basis and $\mathbb{I}$ denotes an identity operator. For probabilistic operations, ρ_{out} is normalized so that its trace is equal to the success probability of $\mathcal{E}$ for input state ρ_{in},

$$p = \text{Tr}\big[\rho_{\text{in}}^T \otimes \mathbb{I}_{\text{out}} \chi\big]. \qquad (7)$$

The Choi matrix of a unitary CZ gate (1) reads

$$\chi_{\text{CZ}} = (\mathbb{I} \otimes U_{\text{CZ}})|\Phi^+\rangle\langle\Phi^+|(\mathbb{I} \otimes U_{\text{CZ}}^\dagger), \qquad (8)$$

hence it is proportional to a density matrix of a pure maximally entangled state. The process fidelity of quantum operation χ with respect to the unitary CZ gate is defined as a normalized overlap of their Choi matrices,

$$F_\chi = \frac{\text{Tr}[\chi \chi_{\text{CZ}}]}{\text{Tr}[\chi_{\text{CZ}}]\text{Tr}[\chi]}. \qquad (9)$$

Sometimes F_χ is called entanglement fidelity [32] because it is defined as an overlap of χ with a pure maximally entangled state.

A. Quantum-process tomography

In our experiment, the CZ gate is probed with 36 product two-qubit states $|\Psi_{jk}\rangle = |\psi_j\rangle|\psi_k\rangle$, where the six different single-qubit states $|\psi_j\rangle$ form three mutually unbiased bases

$$|\psi_j\rangle \in \{|H\rangle, |V\rangle, |D\rangle, |A\rangle, |R\rangle, |L\rangle\}. \qquad (10)$$

The measurements on the output two-photon states are products of single-qubit projective measurements, where each qubit is measured in one of the three bases H/V, D/A, and R/L and we perform two-qubit measurements for all nine combinations of these bases. The probability of projecting the output photons onto state $|\Psi_{lm}\rangle$ for input state $|\Psi_{jk}\rangle$ can be expressed as

$$p_{jk,lm} = \text{Tr}\big[\Psi_{jk}^T \otimes \Psi_{lm} \chi\big]. \qquad (11)$$

The preparation of input probe states together with the measurement on the output states can be interpreted as a quantum measurement on χ, described by a positive operator valued measure (POVM) with 36×36 elements $\Pi_{jk,lm} = \Psi_{jk}^T \otimes \Psi_{lm}$. This POVM satisfies the completeness relation

$$\sum_{j,k=1}^6 \sum_{l,m=1}^6 \Pi_{jk,lm} = 81\mathbb{I} \qquad (12)$$

and the knowledge of all $p_{jk,lm}$ fully and unambiguously determines χ. Note that Eq. (12) implies that

$$\sum_{j,k=1}^6 \sum_{l,m=1}^6 p_{jk,lm} = 81\,\text{Tr}[\chi]. \qquad (13)$$

The measured coincidences $C_{jk,lm}$ exhibit Poissonian statistics with mean equal to $N p_{jk,lm}$, where N is the average number of photon pairs generated by the source during the measurement time of 30 s. We reconstruct the quantum operation χ from the measured coincidences with the help of maximum-likelihood estimation [33,34]. The likelihood function representing the probability of measurement results $C_{jk,lm}$ for a given quantum operation χ can be expressed as

$$\mathcal{L} = \prod_{j,k=1}^6 \prod_{l,m=1}^6 \frac{(N p_{jk,lm})^{C_{jk,lm}}}{C_{jk,lm}!} e^{-N p_{jk,lm}}. \qquad (14)$$

It is convenient to work with the log-likelihood function $\ln\mathcal{L}$. The terms that do not depend on χ can be omitted and using Eq. (13) we obtain

$$\ln\mathcal{L} = \sum_{j,k=1}^6 \sum_{l,m=1}^6 C_{jk,lm} \ln p_{jk,lm} - \lambda \text{Tr}[\chi], \qquad (15)$$

where $\lambda = 81N$. The actual pair generation rate N is unknown due to various losses and imperfect photon collection and detection efficiency. Therefore, $\text{Tr}[\chi]$ can be effectively considered as a free parameter and we can set $\text{Tr}[\chi] = 1$ during the maximization of the log-likelihood function (15). Maximum-likelihood estimation of probabilistic quantum operation then becomes completely equivalent to quantum-state estimation. The quantum operation χ that maximizes $\mathcal{L}$ satisfies the extremal equation [33]

$$R\chi = \lambda\chi, \qquad (16)$$

where

$$R = \sum_{j,k=1}^6 \sum_{l,m=1}^6 \frac{C_{jk,lm}}{p_{jk,lm}} \Pi_{jk,lm}, \qquad (17)$$

and the Lagrange multiplier λ that fixes the trace of χ is proportional to the total number of coincidences $\lambda = C_{\text{tot}}/\text{Tr}[\chi]$, where

$$C_{\text{tot}} = \sum_{j,k=1}^6 \sum_{l,m=1}^6 C_{jk,lm}. \qquad (18)$$

The operation χ that maximizes $\mathcal{L}$ can be calculated by repeated iterations of the symmetrized extremal equation, which preserves the positive semidefiniteness of χ [34],

$$\chi = \frac{R\chi R}{\text{Tr}[R\chi R]}. \qquad (19)$$

As a starting point of the iterations we choose a full-rank operator $\chi_0 = \mathbb{I}/16$ and the iterations are terminated when $|R\chi - \lambda\chi|_1/C_{\text{tot}} < 10^{-5}$, where $|A|_1 = \sum_{j,k} |A_{jk}|$.

B. Monte Carlo sampling

Here we review the estimation of quantum-process fidelity by Monte Carlo sampling as proposed in Refs. [22,23], paying special attention to the fact that we deal with probabilistic trace-decreasing operations. The operator χ_{CZ} defined in Eq. (8) can be expanded in the operator basis formed by tensor products of Pauli matrices

$$\chi_{\text{CZ}} = \sum_{a,b,c,d=0}^3 s_{abcd}\sigma_a \otimes \sigma_b \otimes \sigma_c \otimes \sigma_d. \qquad (20)$$

TABLE I. Nonzero coefficients s_{abcd} in the expression (23) for process fidelity of a quantum CZ gate.

a	b	c	d	s_{abcd}	a	b	c	d	s_{abcd}
0	0	0	0	0.25	2	0	2	3	−0.25
0	1	3	1	0.25	2	1	1	2	0.25
0	2	3	2	−0.25	2	2	1	1	0.25
0	3	0	3	0.25	2	3	2	0	−0.25
1	0	1	3	0.25	3	0	3	0	0.25
1	1	2	2	0.25	3	1	0	1	0.25
1	2	2	1	0.25	3	2	0	2	−0.25
1	3	1	0	0.25	3	3	3	3	0.25

It will be helpful to express the Pauli operators in terms of projectors onto the probe states $|\psi_j\rangle$,

$$
\begin{aligned}
\sigma_0 &= |H\rangle\langle H| + |V\rangle\langle V|, \\
\sigma_1 &= |D\rangle\langle D| - |A\rangle\langle A|, \\
\sigma_2 &= |R\rangle\langle R| - |L\rangle\langle L|, \\
\sigma_3 &= |H\rangle\langle H| - |V\rangle\langle V|.
\end{aligned}
\tag{21}
$$

Due to the orthogonality relations $\mathrm{Tr}[\sigma_a\sigma_b] = 2\delta_{ab}$, the coefficients in the expansion (20) can be determined as

$$
s_{abcd} = \tfrac{1}{16}\mathrm{Tr}[\chi_{CZ}\sigma_a \otimes \sigma_b \otimes \sigma_c \otimes \sigma_d].
\tag{22}
$$

For the CZ gate one finds that only 16 of the coefficients (22) are nonzero [24] and these coefficients are listed in Table I. On inserting the expansion (20) into the formula for F_χ we obtain

$$
F_\chi = \frac{1}{4\,\mathrm{Tr}[\chi]} \sum_{a,b,c,d} s_{abcd}\mathrm{Tr}[\sigma_a \otimes \sigma_b \otimes \sigma_c \otimes \sigma_d \chi].
\tag{23}
$$

If we insert the expressions (21) into Eq. (23) and make use of the identity (13), we find that F_χ can be written as a ratio of linear functions of probabilities $p_{jk,lm}$,

$$
F_\chi = \frac{81}{4} \frac{\sum_{j,k,l,m=1}^{6} u_{jk,lm} p_{jk,lm}}{\sum_{j,k,l,m=1}^{6} p_{jk,lm}},
\tag{24}
$$

where the coefficients $u_{jk,lm}$ are certain linear combinations of s_{abcd}. Note that the expression (24) for F_χ is not unique because the single-qubit identity operator σ_0 can be expressed in different ways in terms of the projectors onto $|\psi_j\rangle$. For instance, instead of formula (21) we can use $\sigma_0 = |D\rangle\langle D| + |A\rangle\langle A|$ or $\sigma_0 = |R\rangle\langle R| + |L\rangle\langle L|$. Also the normalization factor $\mathrm{Tr}[\chi]$ can be expressed in terms of the probabilities $p_{jk,lm}$ in many different ways. Since the (mean values of) measured coincidences $C_{jk,lm}$ are proportional to $p_{jk,lm}$, we can replace the probabilities with coincidences in Eq. (24) to obtain an estimator of the process fidelity

$$
F_{MC} = \frac{81}{4} \frac{\sum_{j,k,l,m=1}^{6} u_{jk,lm} C_{jk,lm}}{\sum_{j,k,l,m=1}^{6} C_{jk,lm}}.
\tag{25}
$$

Since we are able to collect enough data to estimate all terms in the expansion (24), we do not need to perform random sampling of only some of those terms as prescribed by the generic Monte Carlo sampling procedure [22,23]. Note, however, that such random sampling is extremely useful for

large systems because it ensures that the total number of measurements that need to be carried out depends only on the required precision of fidelity estimation and not on the system size [22,23].

C. Hofmann bounds

As shown by Hofmann [10], a lower and upper bound on the process fidelity F_χ can be obtained from average state fidelities evaluated for two mutually unbiased bases. In the case of the CZ gate it is particularly suitable to use the product basis $\{|DH\rangle, |DV\rangle, |AH\rangle, |AV\rangle\}$ and a dual basis obtained from the first basis by a Hadamard transform on each qubit, $\{|HD\rangle, |VD\rangle, |HA\rangle, |VA\rangle\}$. In what follows we shall label these bases as 1 and 2 and we denote by $|\omega_{j,k}\rangle$ a jth state of basis k. The unitary CZ gate transforms all input states $|\omega_{j,k}\rangle$ onto output product states

$$
\begin{aligned}
U_{CZ}|DH\rangle &= |DH\rangle, & U_{CZ}|HD\rangle &= |HD\rangle, \\
U_{CZ}|DV\rangle &= |AV\rangle, & U_{CZ}|VD\rangle &= |VA\rangle, \\
U_{CZ}|AH\rangle &= |AH\rangle, & U_{CZ}|HA\rangle &= |HA\rangle, \\
U_{CZ}|AV\rangle &= |DV\rangle, & U_{CZ}|VA\rangle &= |VD\rangle,
\end{aligned}
\tag{26}
$$

hence the state fidelities can be directly determined by measurements in product two-qubit bases.

The normalized output state of the quantum operation χ for the input $|\omega_{j,k}\rangle$ reads

$$
\rho_{j,k} = \frac{1}{p_{j,k}}\mathrm{Tr}_{\mathrm{in}}\big[\omega_{j,k}^T \otimes \mathbb{I}_{\mathrm{out}}\chi\big],
\tag{27}
$$

where $p_{j,k} = \mathrm{Tr}[\omega_{j,k}^T \otimes \mathbb{I}_{\mathrm{out}}\chi]$ is the success probability of χ for input $|\omega_{j,k}\rangle$ and $\omega_{j,k} = |\omega_{j,k}\rangle\langle\omega_{j,k}|$. The fidelity of the output state $\rho_{j,k}$ is defined as overlap with the pure state $U_{CZ}|\omega_{j,k}\rangle$ produced by the unitary CZ gate,

$$
f_{j,k} = \langle\omega_{j,k}|U_{CZ}^\dagger\rho_{j,k}U_{CZ}|\omega_{j,k}\rangle.
\tag{28}
$$

The average output state fidelity for the kth basis is defined as a weighted mean of $f_{j,k}$ with weights equal to the success probabilities $p_{j,k}$ [18,35],

$$
F_k = \frac{\sum_{j=1}^{4} p_{j,k} f_{j,k}}{\sum_{j=1}^{4} p_{j,k}}.
\tag{29}
$$

Note that in order to determine F_k we do not need the absolute success probabilities but only the relative probabilities $P_{j,k} = p_{j,k}/\sum_{j'} p_{j',k}$.

Let $C_{j,j'}^k$ denote the number of coincidences corresponding to projections onto a product state $U_{CZ}|\omega_{j',k}\rangle$ for input probe state $|\omega_{j,k}\rangle$. The state fidelities and relative success probabilities can be estimated as [18]

$$
f_{j,k} = \frac{C_{j,j}^k}{S_j^k}, \qquad P_{j,k} = \frac{S_j^k}{\sum_{j=1}^{4} S_j^k},
\tag{30}
$$

where $S_j^k = \sum_{j'=1}^{4} C_{j,j'}^k$. On inserting these expressions into Eq. (29) we finally obtain

$$
F_k = \frac{\sum_{j=1}^{4} C_{j,j}^k}{\sum_{j=1}^{4} S_j^k}.
\tag{31}
$$

In the case of perfect gate operation only $C_{j,j}^k$ would be nonzero and $C_{j,j'}^k = 0$ if $j \neq j'$. The average fidelity (31) is thus given by a ratio of the sum of the "good" coincidences $C_{j,j}^k$ and the sum of all the coincidences $C_{j,j'}^k$.

Since $\sum_{j=1}^4 \omega_{j,k} = \mathbb{I}$ for all k, it holds that $\sum_{j=1}^4 p_{j,k} = \text{Tr}[\chi]$ and we can express the mean fidelities defined in Eq. (29) in a compact matrix form $F_k = \text{Tr}[Q_k \chi]/\text{Tr}[\chi]$, where

$$Q_k = \sum_{j=1}^4 \omega_{j,k}^T \otimes \left(U_{\text{CZ}} \omega_{j,k} U_{\text{CZ}}^\dagger\right). \qquad (32)$$

The gate fidelity F_χ can be bounded by the average state fidelities as [10,18]

$$\min(F_1, F_2) \geqslant F_\chi \geqslant F_1 + F_2 - 1 \equiv F_H. \qquad (33)$$

With the help of the above expressions one can rewrite the lower bound condition as

$$\frac{\text{Tr}[Q\chi]}{\text{Tr}[\chi]} \geqslant 0, \qquad (34)$$

where $Q = \frac{1}{4}\chi_{\text{CZ}} - Q_1 - Q_2 + \mathbb{I}$. It can be shown by explicit calculation that the operator Q is positive semidefinite, which proves that the inequality (34) holds for both deterministic and probabilistic quantum operations χ [18].

If all success probabilities $p_{j,k}$ are equal then the weighted means can be replaced by the ordinary means $\bar{F}_k = \frac{1}{4}\sum_{j=1}^4 f_{j,k}$ and we obtain the Hofmann bound as originally formulated for deterministic operations

$$F_\chi \geqslant \bar{F}_1 + \bar{F}_2 - 1 \equiv F_D. \qquad (35)$$

We emphasize that this latter bound does not hold for probabilistic operations and $\bar{F}_1 + \bar{F}_2 - 1$ may be larger than F_χ if χ is a trace-decreasing map. In order to compare the two bounds (33) and (35) we write

$$f_{j,k} = \bar{F}_k + \Delta f_{j,k}, \quad p_{j,k} = \bar{p} + \Delta p_{j,k}, \qquad (36)$$

where $\bar{p} = \sum_j p_{j,k}/4 = \text{Tr}[\chi]/4$. Since $\sum_j \Delta f_{j,k} = 0$ and $\sum_j \Delta p_{j,k} = 0$ by definition, we have

$$F_1 + F_2 = \bar{F}_1 + \bar{F}_2 + \frac{1}{4\bar{p}} \sum_{j=1}^4 (\Delta p_{j,1} \Delta f_{j,1} + \Delta p_{j,2} \Delta f_{j,2}). \qquad (37)$$

This formula reveals that the bounds (33) and (35) will differ considerably only if the state fidelities $f_{j,k}$ and success probabilities $p_{j,k}$ exhibit significant variations.

IV. MODEL OF A LINEAR OPTICAL CZ GATE

To experimentally probe various regimes of the gate operation including the situation where the success probabilities significantly depend on the input states, we deliberately introduce a variable time delay between the photons with the help of a delay line (see Fig. 1). The time delay makes the photons partially or even fully distinguishable and it thus reduces the visibility of their interference [36]. In this section we analyze theoretically the impact of the reduced visibility of two-photon interference on the behavior of the gate. We will model this situation in a simple way: We assume that the two

photons either interfere with probability q or behave as perfectly distinguishable particles with probability $1 - q$. A more detailed model including also errors in the transmittance of the partially polarizing beam splitters can be found in Ref. [37].

It is instructive to relate the value of the parameter q to the visibility of Hong-Ou-Mandel (HOM) interference that can be directly measured experimentally. If we prepare a signal photon in state $|V\rangle$ and an idler photon in state $|H\rangle$ and set the waveplates in the second qubit analysis block such that it performs a measurement in the D/A basis, then a HOM dip can be observed by measuring the coincidences between detectors D3 and D4. The observed coincidence rate C will be proportional to the photons' distinguishability $C = C_\infty(1 - q)$, where C_∞ is the rate outside the dip. Visibility of two-photon interference is defined as $\mathcal{V} = (C_\infty - C)/(C_\infty + C)$ and after some algebra we obtain the relation

$$q = \frac{2\mathcal{V}}{1 + \mathcal{V}}. \qquad (38)$$

The operation of the gate can be seen as a probabilistic mixture with probability q of a perfect operation of the CZ gate (when the photons perfectly interfere and the gate succeeds with probability $1/9$) and of an incoherent transformation χ_{inc} occurring otherwise. Thus, the Choi-Jamiolkowski operator corresponding to the gate reads

$$\chi = \frac{q}{9} \chi_{\text{CZ}} + (1 - q)\chi_{\text{inc}}. \qquad (39)$$

If the photons are distinguishable then the gate operation still succeeds if both photons are either transmitted through or reflected from the central PPBS, but these two contributions become distinguishable and have to be added together incoherently. After some algebra we thus find that χ_{inc} is a mixture of an identity channel and an operation corresponding to projection onto state $|VV\rangle$,

$$\chi_{\text{inc}} = \frac{1}{9}|\Phi^+\rangle\langle\Phi^+| + \frac{4}{9}|VVVV\rangle\langle VVVV|, \qquad (40)$$

where we recall that

$$|\Phi^+\rangle = |HHHH\rangle + |HVHV\rangle + |VHVH\rangle + |VVVV\rangle \qquad (41)$$

in our current notation. The dependence of the gate fidelity on visibility $\mathcal{V}$ can be determined using Eqs. (38) and (39) and we get

$$F_\chi = \frac{1 + 3\mathcal{V}}{4}. \qquad (42)$$

We can see that the gate operates perfectly for $\mathcal{V} = 1$ (or equivalently $q = 1$) and has fidelity $1/4$ if we operate it out of the HOM interference ($\mathcal{V} = q = 0$).

Let us now investigate the dependence of the Hofmann bound on the interference visibility. Our goal is to calculate the mean state fidelities F_k and $\bar{F}_k$ and for this purpose we need to evaluate $p_{j,k}$ and $f_{j,k}$ as defined in Sec. III C. It is convenient to rewrite the expression for success probability as $p_{j,k} = \text{Tr}[\omega_{j,k}^T X]$, where

$$X = \text{Tr}_{\text{out}}[\chi] = \frac{1}{9}\mathbb{I} + \frac{4}{9}(1 - q)|VV\rangle\langle VV|. \qquad (43)$$

The four probe states $|HD\rangle$, $|HA\rangle$, $|DH\rangle$, and $|AH\rangle$ have $|0\rangle \equiv |H\rangle$ as one of the qubits and the ideal CZ gate would act

as an identity on them. Moreover, all these states are orthogonal to $|VV\rangle$. Therefore, we have for all these states

$$p_{j,k} = \tfrac{1}{9}, \quad f_{j,k} = 1, \tag{44}$$

irrespective of the value of visibility $\mathcal{V}$. On the other hand, the remaining four input states $|VD\rangle$, $|VA\rangle$, $|DV\rangle$, and $|AV\rangle$ have an overlap $1/\sqrt{2}$ with $|VV\rangle$ and we get

$$p_{j,k} = \frac{3-2q}{9}, \quad f_{j,k} = \frac{1}{3-2q} \tag{45}$$

for all of them.

At this stage we are ready to evaluate F_k and $\bar{F}_k$. Since each basis contains two states from the first and two states from the second above-mentioned groups of states, we get

$$F_1 = F_2 = \frac{1+\mathcal{V}}{2}, \quad \bar{F}_1 = \bar{F}_2 = \frac{2}{3-\mathcal{V}}. \tag{46}$$

The Hofmann bound (33) implies that the gate fidelity should satisfy

$$\mathcal{V} \leqslant F_\chi \leqslant \frac{1+\mathcal{V}}{2}, \tag{47}$$

hence the lower bound on F_χ is directly equal to the visibility of two-photon interference $\mathcal{V}$. It is easy to see that the true fidelity (42) indeed satisfies the inequalities (47) as it should. In Fig. 2 we plot the true process fidelity as well as the Hofmann lower bound in dependence on the interference visibility $\mathcal{V}$.

If we use the ordinary average state fidelities $\bar{F}_k$ instead of the weighted averages F_k, then we get

$$F_D \equiv \bar{F}_1 + \bar{F}_2 - 1 = \frac{1+\mathcal{V}}{3-\mathcal{V}}, \tag{48}$$

which is larger than the true fidelity F_χ when $\mathcal{V} < \frac{1}{3}$ (see Fig. 2). This explicitly demonstrates that the lower bound (35) is guaranteed to work only for deterministic operations and its application to probabilistic operations may lead to overestimation of the process fidelity. Since $F_D - F_H = (1 - \mathcal{V})^2/(3-\mathcal{V})$, the two bounds become very similar for high
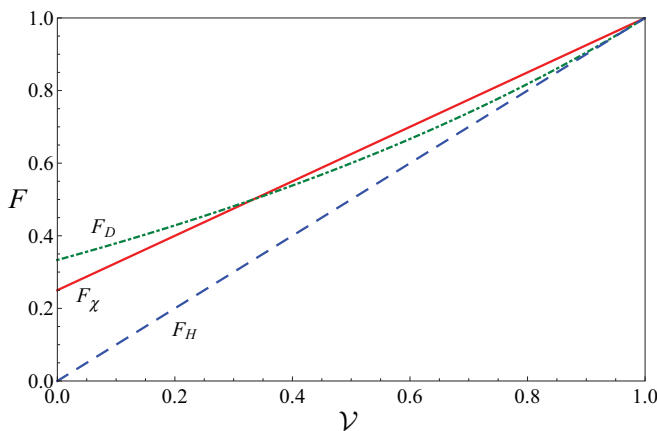

FIG. 2. (Color online) Dependence of the gate fidelity F_χ (solid red line), lower bound on gate fidelity F_H (blue dashed line), and lower bound valid for deterministic operations F_D (green dot-dashed line) on two-photon interference visibility $\mathcal{V}$.

interference visibilities and the difference becomes significant only for relatively low visibility (see Fig. 2).

V. RESULTS

The tomographically complete measurements specified in Sec. III were performed for three different values of visibility of the two-photon interference $\mathcal{V}$. The first measurement was carried out at the Hong-Ou-Mandel dip where $\mathcal{V} = 0.953$, which is the maximum visibility that we achieved with our setup. The second measurement was carried out with partly distinguishable photons ($\mathcal{V} = 0.50$) and for the third measurement the temporal delay between the photons was increased such that they became completely distinguishable ($\mathcal{V} = 0.022$).

The quantum-process matrices determined by the maximum-likelihood estimation procedure are plotted in Fig. 3. We can see that the shape of the reconstructed process matrices is in good agreement with the theoretical predictions for all the visibilities. In Table II we summarize the quantum-process fidelities F_χ determined from the reconstructed quantum-process matrices. The table also contains process fidelities F_{MC} estimated by Monte Carlo sampling and the Hofmann lower bound (33) on process fidelity F_H. For comparison, the table also includes a lower bound on process fidelity F_D that is valid only for deterministic operations [see Eq. (35)]. The coincidences and relative success probabilities required for evaluation of F_H and F_D are plotted in Fig. 4. The data are in good agreement with the prediction of the theoretical model described in Sec. IV. In particular, all the success probabilities are almost identical at the dip, while well outside the dip the states split into two groups whose success probabilities differ almost by a factor of 3.

The statistical uncertainty of F_{MC}, F_H, and F_D was estimated assuming Poissonian statistics of the measured coincidences and using standard error propagation. After some algebra we find that the statistical uncertainty of the Monte Carlo fidelity estimate F_{MC} can be expressed as

$$(\Delta F_{MC})^2 = \frac{1}{C_{tot}} \sum_{j,k,l,m=1}^{6} \frac{C_{jk,lm}}{C_{tot}} \left(\frac{81}{4} u_{jk,lm} - F_{MC} \right)^2 \tag{49}$$

and the statistical uncertainty of the Hofmann bounds is given by

$$(\Delta F_H)^2 = \sum_{k=1}^{2} \frac{F_k(1-F_k)}{\sum_{j=1}^{4} S_j^k},$$

$$(\Delta F_D)^2 = \frac{1}{16} \sum_{k=1}^{2} \sum_{j=1}^{4} \frac{f_{j,k}(1-f_{j,k})}{S_j^k}. \tag{50}$$

In order to estimate the statistical uncertainty of fidelity F_χ determined from the reconstructed process matrix χ, we have performed repeated simulations of the experiment followed by maximum-likelihood reconstruction of the process matrix. For each $\mathcal{V}$ this procedure yielded an ensemble of 100 reconstructed quantum-process matrices and a corresponding ensemble of process fidelities whose spread as quantified by one standard deviation was consistently lower than 10^{-3}. The
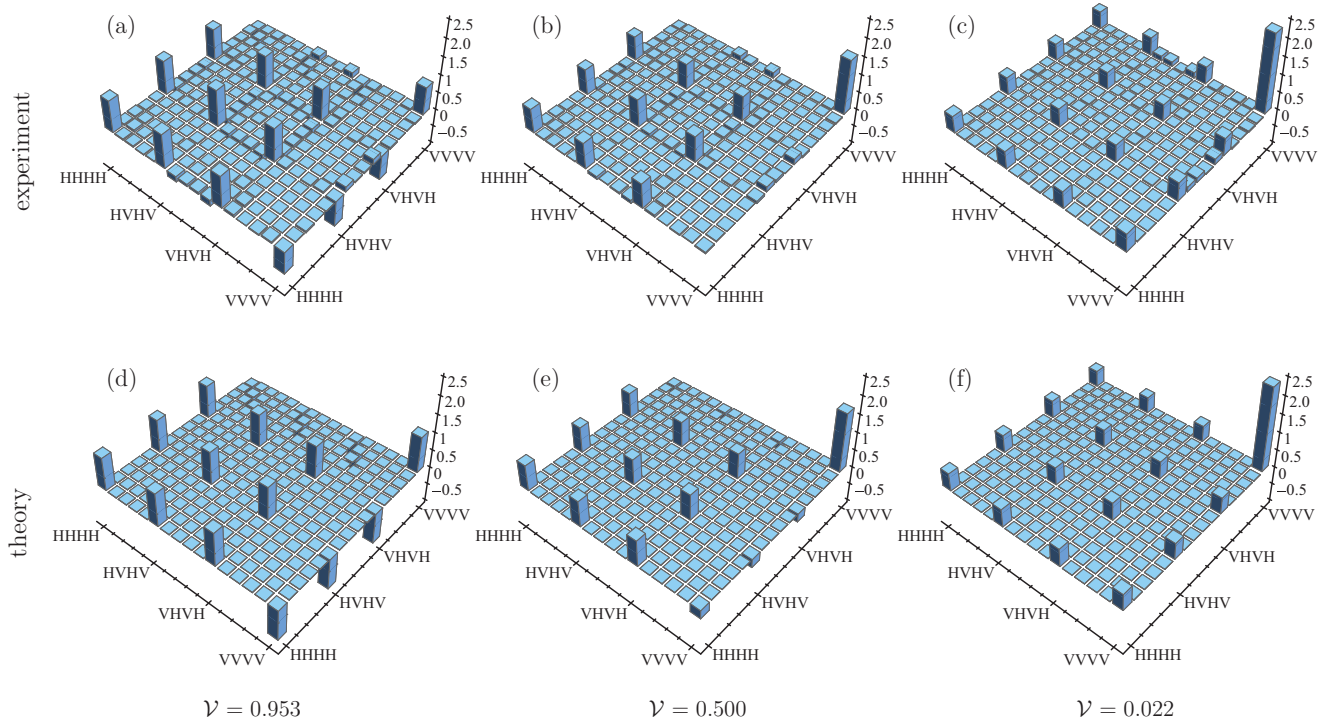
FIG. 3. (Color online) (a)–(c) quantum-process matrices χ of a linear optical CZ gate determined by maximum-likelihood reconstruction from experimental data and (d)–(f) theoretical process matrices determined from the model presented in Sec. IV. The results are shown for three values of two-photon interference visibility (a) and (d) $\mathcal{V} = 0.953$, (b) and (e) $\mathcal{V} = 0.50$, and (c) and (f) $\mathcal{V} = 0.022$. Imaginary parts of reconstructed χ represent a small noise background and are not plotted. To facilitate comparison, all matrices are normalized such that $\mathrm{Tr}[\chi] = 4$.

statistical uncertainty of F_χ indicated in Table II therefore represents a conservative upper bound.

The experimentally determined process fidelities F_χ and F_{MC} are somewhat smaller than the fidelity $(1 + 3V)/4$ predicted by the theoretical model. This can be partly explained by the imperfections of the three partially polarizing beam splitters [37] whose measured transmittances $T_{H1} = 0.983$, $T_{V1} = 0.348$, $T_{H2} = 0.983$, $T_{V2} = 0.344$, $T_{H3} = 0.984$, and $T_{V3} = 0.324$ differ slightly from the ideal values $T_H = 1$ and $T_V = 1/3$. Note also that the differences between maximum-likelihood and Monte Carlo estimates are larger than statistical uncertainty. Moreover, in the high-visibility regime $\mathcal{V} = 0.95$ the Hofmann lower bound F_H exceeds both F_χ and F_{MC} by an amount that is larger than the statistical error. All these features indicate the influence of some effects that introduce systematic errors. To further investigate this aspect of our experiment,

we have determined Monte Carlo estimates of the process fidelity using three different estimators. These estimators were

TABLE II. Experimentally determined quantum-process fidelities F_χ and F_{MC}, Hofmann lower bound on process fidelity F_H, lower bound F_D valid for deterministic operations, and upper bound on process fidelity provided by the minimum of average state fidelities F_1 and F_2. The results are shown for three values of visibility $\mathcal{V}$.

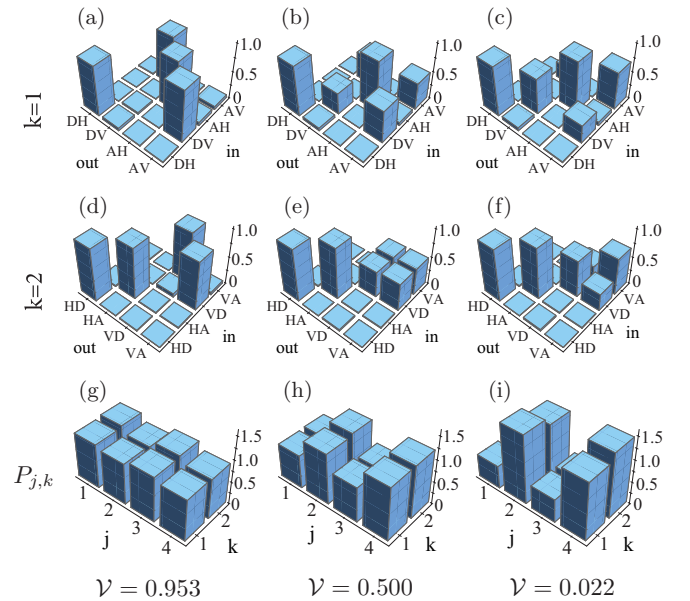| $\mathcal{V}$	F_D	F_H	F_χ	F_{MC}	$\min(F_1, F_2)$
0.953	0.875(2)	0.877(2)	0.860(1)	0.871(2)	0.934(1)
0.500	0.465(2)	0.372(2)	0.531(1)	0.539(1)	0.676(1)
0.022	0.253(2)	−0.034(2)	0.232(1)	0.252(1)	0.479(1)

FIG. 4. (Color online) (a)–(f) Normalized coincidences $C_{j,j'}^k/S_j^k$ and (g)–(i) relative success probabilities $P_{j,k}$ used for determination of the Hofmann bound on the quantum-process fidelity. The results are shown for the three visibilities (a), (d), and (g) $\mathcal{V} = 0.953$, (b), (e), and (h) $\mathcal{V} = 0.500$, and (c), (f), and (i) $\mathcal{V} = 0.022$.

TABLE III. Monte Carlo estimates of quantum-process fidelity determined from the original and renormalized coincidences are listed for the three considered values of interference visibility $\mathcal{V}$ and three different expansions of the single-qubit identity operator σ_0 leading to different Monte Carlo estimators.

$\mathcal{V}$	σ_0	F_{MC}	$\tilde{F}_{MC}$
0.953	H/V	0.871(2)	0.861(2)
0.953	D/A	0.882(2)	0.870(2)
0.953	R/L	0.833(1)	0.846(1)
0.500	H/V	0.539(1)	0.533(2)
0.500	D/A	0.521(1)	0.518(2)
0.500	R/L	0.515(1)	0.520(1)
0.022	H/V	0.252(1)	0.240(1)
0.022	D/A	0.245(1)	0.240(1)
0.022	R/L	0.242(1)	0.235(1)

obtained following the procedure described in detail in Sec. III B, where the single-qubit identity operator was expressed in three different ways as a sum of projectors $\sigma_0 = |H\rangle\langle H| + |V\rangle\langle V|$, $\sigma_0 = |D\rangle\langle D| + |A\rangle\langle A|$, or $\sigma_0 = |R\rangle\langle R| + |L\rangle\langle L|$. The results are summarized in Table III. We can see that the three estimators lead to fidelity estimates that differ by amounts exceeding the statistical uncertainty and the differences are largest in the high-visibility regime of operation.

Given the long duration of data acquisition (almost 17 h for each fixed $\mathcal{V}$), the measurements can be affected by long-term fluctuations of the rate of our source of correlated photon pairs. In order to track these fluctuations, we have performed additional coincidence measurements that can be used for data calibration. For each of the 36 input states $|\Psi_{jk}\rangle$ we have measured the 36 coincidences $C_{jk,lm}$ and then we measured reference coincidences D_{jk} for a fixed setting that did not depend on j,k (input state $|HH\rangle$, projection onto $|HH\rangle$). The dependence of the reference coincidences D_{jk} on time is plotted in Fig. 5. The observed long-term fluctuations are indeed non-negligible and should be accounted
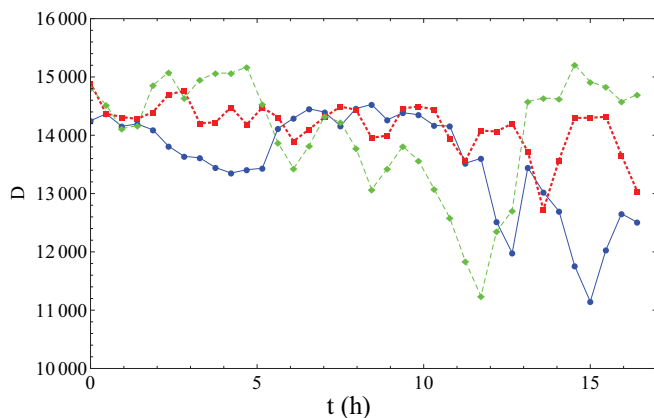

FIG. 5. (Color online) Reference coincidences D_{jk} plotted as a function of time for the three considered two-photon visibilities $\mathcal{V} = 0.953$ (solid blue line), $\mathcal{V} = 0.50$ (red dotted line), and $\mathcal{V} = 0.022$ (green dashed line).

for in data processing. We therefore renormalize the measured coincidences

$$\tilde{C}_{jk,lm} = \frac{C_{jk,lm}}{D_{jk}}. \tag{51}$$

Monte Carlo estimates of process fidelity $\tilde{F}_{MC}$ obtained from the renormalized coincidences are listed in the last column of Table III. The data calibration leads to a reduction of the spread of the three estimates for each fixed visibility $\mathcal{V}$. The calibration (51) modifies the statistical uncertainty of the estimates because the reference coincidences D_{jk} are fluctuating quantities. Following the same procedure as before, we find that the statistical error of $\tilde{F}_{MC}$ is given by

$$(\Delta \tilde{F}_{MC})^2 = \frac{1}{\tilde{C}_{tot}^2} \sum_{j,k,l,m=1}^{6} \frac{\tilde{C}_{jk,lm}}{D_{j,k}} \left(\frac{81}{4} u_{jk,lm} - \tilde{F}_{MC} \right)^2$$

$$+ \frac{1}{\tilde{C}_{tot}^2} \sum_{j,k=1}^{6} \frac{1}{D_{jk}} \left[\sum_{l,m=1}^{6} \tilde{C}_{jk,lm} \left(\frac{81}{4} u_{jk,lm} - \tilde{F}_{MC} \right) \right]^2. \tag{52}$$

Explicit calculations reveal that the contribution due to fluctuations of D_{jk} is almost negligible and the statistical uncertainty of $\tilde{F}_{MC}$ is of the order of 10^{-3}, similar to that for F_{MC} (see Table III).

Using the renormalized coincidences (51), we have also evaluated the Hofmann bounds F_H and F_D and the process fidelity F_χ obtained from the process matrix χ determined by maximum-likelihood reconstruction. It turns out that, in contrast to Monte Carlo sampling, the renormalization has a negligible impact on these fidelity values. The largest difference occurs for F_χ at the high-visibility regime ($\mathcal{V} = 0.95$) where we get $F_\chi = 0.860$ before renormalization and $F_\chi = 0.858$ after renormalization. In all other cases, the difference between fidelities obtained from the original coincidences and the renormalized coincidences is smaller than 0.002. Let us outline a possible explanation of this robustness with respect to fluctuations of the pair generation rate. Since all measurements for any given input state were performed in a row in a relatively short time span of approximately 30 min, the long-term fluctuations of the source rate have only a small impact on the estimation of state fidelities $f_{j,k}$ that appear in expressions for F_H and F_D. On the other hand, the maximum-likelihood estimation combines together all the data that form a significantly overcomplete set and therefore it in a sense averages over the long-term fluctuations of the source.

This analysis shows that the long-term fluctuations of the pair generation rate do not completely explain the observed discrepancies between the fidelities. We therefore conclude that these discrepancies are caused by other systematic effects. One such phenomenon could be a change of the visibility of two-photon interference during the measurement. This is supported by the fact that the observed fidelity discrepancies are largest in the high-visibility regime. In this case the setup is initially tuned to maximum visibility and thermal drifts and other effects cause a reduction of the visibility in the course of the measurement. By contrast, if the setup is operated with large temporal delay between the two photons then small random changes of this delay do not have any impact on

the performance of the scheme. Another possible source of systematic errors consists in imperfections of the waveplates and polarizing beam splitters that serve for state preparation and analysis.

VI. CONCLUSION

In summary, we have compared several methods of quantum-process-fidelity estimation using the linear optical CZ gate as a suitable testing platform. We have considered a linear fidelity estimator based on the Monte Carlo sampling as well as a nonlinear estimator based on maximum-likelihood reconstruction of the full process matrix χ. In addition, we have also evaluated lower bounds on quantum-process fidelity provided by average quantum-state fidelities. Since we have used the same data set to evaluate all the fidelities, the results admit direct comparison. We have observed good agreement between the Monte Carlo and maximum-likelihood estimates and also the fidelity bounds F_H and F_D behaved according to theoretical predictions. The observed small discrepancies between F_{MC} and F_χ can be partly attributed to fluctuations of the photon-pair generation rate in the course of measurement, which were tracked by performing reference measurements and compensated for by renormalization of the measured coincidences.

The remaining residual discrepancies between fidelity estimates can be attributed to various systematic effects such as change of the two-photon interference visibility during the measurement or small imperfections of the waveplates and polarizing beam splitters that are used for state preparation and analysis. In this context it is worth mentioning that it was shown very recently that fidelity estimation based on maximum-likelihood reconstruction may lead to systematic underestimation of the fidelity [38]. This underlies the importance of other more direct fidelity estimation techniques such as Monte Carlo sampling or fidelity bounds based on average state fidelities.

By tuning the time delay between the two photons, we were able to control the visibility of the two-photon interference and operate the gate in different regimes. In particular, when operated far outside the dip, the gate exhibits very low fidelity and a significant dependence of success probability on the input state. This flexibility allowed us to probe experimentally the influence of the varying success probabilities on the Hofmann lower bound on quantum-process fidelity. For probabilistic gates, a valid lower bound F_H can be obtained with the help of weighted averages of state fidelities with weights represented by the relative success probabilities. In contrast, the bound based on ordinary averages of state fidelities is valid only for deterministic operations and may fail to provide a lower bound for probabilistic operations. This is clearly demonstrated by our theoretical calculations and confirmed also by our experimental data. Well outside the dip we observe $F_D = 0.253(2)$, while $F_\chi = 0.232(1)$ and $\tilde{F}_{MC} \leqslant 0.240(1)$. On the other hand, when the CZ gate is operated at the dip ($\mathcal{V} = 0.95$), then the success probabilities are almost the same for all inputs and F_D and F_H practically coincide. This confirms that the lower bounds on process fidelity of linear optical quantum gates reported in previous works [12–17] are reliable even if they were determined using ordinary averages of the state fidelities.

[1] J. F. Poyatos, J. I. Cirac, and P. Zoller, Phys. Rev. Lett. **78**, 390 (1997).

[2] I. L. Chuang and M. A. Nielsen, J. Mod. Opt. **44**, 2455 (1997).

[3] J. Fiurášek and Z. Hradil, Phys. Rev. A **63**, 020101(R) (2001).

[4] *Quantum State Estimation*, edited by M. Paris and J. Řeháček, Lecture Notes in Physics Vol. 649 (Springer, Heidelberg, 2004).

[5] A. Jamiolkowski, Rep. Math. Phys. **3**, 275 (1972).

[6] M.-D. Choi, Linear Algebra Appl. **10**, 285 (1975).

[7] J. L. O'Brien, G. J. Pryde, A. Gilchrist, D. F. V. James, N. K. Langford, T. C. Ralph, and A. G. White, Phys. Rev. Lett. **93**, 080502 (2004).

[8] D. Gross, Y.-K. Liu, S. T. Flammia, S. Becker, and J. Eisert, Phys. Rev. Lett. **105**, 150401 (2010).

[9] A. Shabani, R. L. Kosut, M. Mohseni, H. Rabitz, M. A. Broome, M. P. Almeida, A. Fedrizzi, and A. G. White, Phys. Rev. Lett. **106**, 100401 (2011).

[10] H. F. Hofmann, Phys. Rev. Lett. **94**, 160504 (2005).

[11] D. M. Reich, G. Gualdi, and C. P. Koch, Phys. Rev. A **88**, 042309 (2013).

[12] R. Okamoto, H. F. Hofmann, S. Takeuchi, and K. Sasaki, Phys. Rev. Lett. **95**, 210506 (2005).

[13] X. H. Bao, T. Y. Chen, Q. Zhang, J. Yang, H. Zhang, T. Yang, and J. W. Pan, Phys. Rev. Lett. **98**, 170502 (2007).

[14] A. S. Clark, J. Fulconis, J. G. Rarity, W. J. Wadsworth, and J. L. O'Brien, Phys. Rev. A **79**, 030303(R) (2009).

[15] W. B. Gao, P. Xu, X.-C. Yao, O. Gühne, A. Cabello, C.-Y. Lu, C.-Z. Peng, Z. B. Chen, and J. W. Pan, Phys. Rev. Lett. **104**, 020501 (2010).

[16] W. B. Gao, A. M. Goebel, C. Y. Lu, H. N. Dai, C. Wagenknecht, Q. A. Zhang, B. Zhao, C. Z. Peng, Z. B. Chen, Y. A. Chen, and J. W. Pan, Proc. Natl. Acad. Sci. USA **107**, 20869 (2010).

[17] X. Q. Zhou, T. C. Ralph, P. Kalasuwan, M. Zhang, A. Peruzzo, B. P. Lanyon, and J. L. O'Brien, Nat. Commun. **2**, 413 (2011).

[18] M. Mičuda, M. Sedlák, I. Straka, M. Miková, M. Dušek, M. Ježek, and J. Fiurášek, Phys. Rev. Lett. **111**, 160407 (2013).

[19] B. P. Lanyon, C. Hempel, D. Nigg, M. Müller, R. Gerritsma, F. Zähringer, P. Schindler, J. T. Barreiro, M. Rambach, G. Kirchmair, M. Hennrich, P. Zoller, R. Blatt, and C. F. Roos, Science **334**, 57 (2011).

[20] J. Emerson, M. Silva, O. Moussa, C. Ryan, M. Laforest, J. Baugh, D. G. Cory, and R. Laflamme, Science **317**, 1893 (2007).

[21] C. Dankert, R. Cleve, J. Emerson, and E. Livine, Phys. Rev. A **80**, 012304 (2009).

[22] S. T. Flammia and Y.-K. Liu, Phys. Rev. Lett. **106**, 230501 (2011).

[23] M. P. da Silva, O. Landon-Cardinal, and D. Poulin, Phys. Rev. Lett. **107**, 210404 (2011).

[24] L. Steffen, M. P. da Silva, A. Fedorov, M. Baur, and A. Wallraff, Phys. Rev. Lett. **108**, 260506 (2012).

[25] P. Kok, W. J. Munro, K. Nemoto, T. C. Ralph, J. P. Dowling, and G. J. Milburn, Rev. Mod. Phys. **79**, 135 (2007).

[26] M. Ježek, I. Straka, M. Mičuda, M. Dušek, J. Fiurášek, and R. Filip, Phys. Rev. Lett. **107**, 213602 (2011).

[27] N. K. Langford, T. J. Weinhold, R. Prevedel, K. J. Resch, A. Gilchrist, J. L. O'Brien, G. J. Pryde, and A. G. White, Phys. Rev. Lett. **95**, 210504 (2005).

[28] N. Kiesel, C. Schmid, U. Weber, R. Ursin, and H. Weinfurter, Phys. Rev. Lett. **95**, 210505 (2005).

[29] K. Lemr, A. Černoch, J. Soubusta, K. Kieling, J. Eisert, and M. Dušek, Phys. Rev. Lett. **106**, 013602 (2011).

[30] T. C. Ralph, N. K. Langford, T. B. Bell, and A. G. White, Phys. Rev. A **65**, 062324 (2002).

[31] H. F. Hofmann and S. Takeuchi, Phys. Rev. A **66**, 024308 (2002).

[32] M. Horodecki, P. Horodecki, and R. Horodecki, Phys. Rev. A **60**, 1888 (1999).

[33] Z. Hradil, Phys. Rev. A **55**, R1561 (1997).

[34] M. Ježek, J. Fiurášek, and Z. Hradil, Phys. Rev. A **68**, 012305 (2003).

[35] B. Bell, A. S. Clark, M. S. Tame, M. Halder, J. Fulconis, W. J. Wadsworth, and J. G. Rarity, New J. Phys. **14**, 023021 (2012).

[36] M. Miková, H. Fikerová, I. Straka, M. Mičuda, M. Ježek, M. Dušek, and R. Filip, Phys. Rev. A **87**, 042327 (2013).

[37] T. Nagata, R. Okamoto, H. F. Hofmann, and S. Takeuchi, New J. Phys. **12**, 043053 (2009).

[38] C. Schwemmer, L. Knips, D. Richart, T. Moroder, M. Kleinmann, O. Gühne, and H. Weinfurter, arXiv:1310.8465.